Carbohydrate Polymers 111 (2014) 469–476

Contents lists available at ScienceDirect

Carbohydrate Polymers

journal homepage: www.elsevier.com/locate/carbpol

Recycled chitosan nanofibril as an effective Cu(II), Pb(II) and Cd(II) ionic chelating agent: Adsorption and desorption performance

Dagang Liu [a,*], Zehui Li [a], Yi Zhu [a], Zhenxuan Li [a], Rakesh Kumar [b]

[a] Department of Chemistry, Jiangsu Key Laboratory of Atmospheric Environment Monitoring and Pollution Control, Nanjing University of Information Science & Technology, Nanjing 210044, China
[b] Department of Applied Chemistry, Birla Institute of Technology, Mesra, Patna Campus, Patna 800014, India

ARTICLE INFO

Article history:
Received 5 February 2014
Received in revised form 8 April 2014
Accepted 10 April 2014
Available online 19 April 2014

Keywords:
Chitosan nanofibrils
Adsorption
Metal ions
Desorption

ABSTRACT

Mechanically disassembled chitosan nanofibrils were prepared and used as metal ion chelating agents. Structure and morphology of nanofibrils were investigated and ionic adsorption or desorption performance were validated to establish related fitting models. In single metal ion solution, the saturated adsorption capacities of Cu(II), Pb(II), Cd(II), Zn(II), and Ni(II) were 168.66, 118.00 and 60.85, 143.67, and 63.32 mg/g, respectively. In ternary metal ion solution, Cu(II) was more competitive to be adsorbed than Pb(II) and Cd(II) and its removal could arrive at 60%. Ions adsorbed by nanofibrils could be released by EDTA and the recovery could keep above 70% after 3 sorption–desorption cycles. Hence, renewable and recyclable nanofibrillar chitosan exhibited a great promising application in metal treatments attributed to its high adsorption capacity and chelation efficiency.

© 2014 Elsevier Ltd. All rights reserved.

1. Introduction

Heavy metals or transition metals emanated from chemical industries are transferred and enriched in water or soil environments (Jeon & Ha Park, 2005; Wang et al., 2010), whereas bring serious problems to living beings (Deng, Liu, Zeng, Qiu, & Li, 2013). Renewable natural resources have been gaining prominence as effective and economical biosorbents to remove toxic metal ions from aqueous environment (Laus & de Fávere, 2011; Muzzarelli, 2011), since these cost-effective adsorbents are known to have high binding capacity on metal ions (Jeon & Ha Park, 2005; Muzzarelli & Sipos, 1971) and many other advantages such as low generation of residues, easy metal recovery, and the possibility of reuse. Chitosan, a partially deacetylated product of chitin, is soluble in acidic media and thereby produces a unique polycationic structure (Gamage & Shahidi, 2007; Popuri, Vijaya, Boddu, & Abburi, 2009; Muzzarelli, Ferrero, & Pizzoli, 1972). It is well known that chitosan is very useful in the aqueous-phase separation of heavy metals (Chen, Liu, Chen, & Chen, 2008; Muzzarelli, 1973; Wan Ngah, Teong, & Hanafiah, 2011).

Environmental fibrillar nanomaterial is one of the most important research topics in recent years due to their interesting characteristics, such as fine diameters (ranging from submicron to several nanometers), large surface area per unit mass, wide-range porosity, high gas permeability, and small interfibrous pore size (Haider & Park, 2009; Liu, Chang, Chen, & Wu, 2011; Muzzarelli, 2012). In our former reports, we established a joint mechanical method to defibrillate chitosan or chitin particles into nanofibrils (Liu, Wu, Chang, & Gao, 2011). In continuation with the earlier studies on chitin nanofibrillar adsorbents (Liu, Zhu, et al., 2013), the chitosan nanofibrils was isolated and used as chelating agents of Cu(II), Pb(II) and Cd(II) ions in this work. The adsorption and desorption performance in single and ternary metal ion system was investigated. We tried to provide some meaningful information about this novel chelating agent by predicting the nature of the adsorption and desorption process for further engineering application in metal pollutant treatments.

2. Experimental

2.1. Materials

Chitosan, with a degree of deacetylation of 90% and average molecular weight of 161 kDa was purchased from Sinopharm Chemical Reagent Co. Ltd (Shanghai, China). The working standard solutions of Cu(II), Pb(II), Cd(II), Zn(II), and Ni(II) were prepared by using appropriate dilutions of stock solutions (500 mg/L), which were configured by cupric(II) nitrate, lead(II) nitrate, cadmium(II) nitrate tetrahydrate, zinc(II) nitrate and nickel(II) nitrate,

* Corresponding author. Tel.: +86 2558731090; fax: +86 2558731090.
E-mail addresses: dagangliu@gmail.com, dagang@nuist.edu.cn (D. Liu).

http://dx.doi.org/10.1016/j.carbpol.2014.04.018
0144-8617/© 2014 Elsevier Ltd. All rights reserved.

Nomenclature

AAS	flame atomic absorption spectroscopy
q	amount of adsorbed metal ions (mg/g)
q_d	amount of desorbed metal ions (mg/g)
q_e	amount of adsorbed ions at equilibrium (mg/g)
q_t	amounts of ions adsorbed at time t (mg/g)
q_m	maximum adsorption capacity (mg/g)
$q_{e\ (exp.)}$	experimental sorption capacity (mg/g)
$q_{e\ (theor.)}$	theoretical sorption capacity (mg/g)
C_o	initial metal concentration (mg/L)
C_e	concentration of equilibrium ion solution (mg/L)
V	volume of the solution (L)
m	mass of adsorbent used (g)
D	percentage of metal ions desorbed
ΔH^0	standard enthalpy change
ΔG^0	Gibbs free energy change
ΔS^0	standard entropy change
T	temperature in Kelvin
R	universal gas constant (8.314 J mol^{-1} K^{-1})
K_L	Langmuir constant
R_L	separation factor or equilibrium parameter
K_F	Freundlich isotherm constants
n	adsorption intensity
k_1	rate constant of pseudo-first order kinetic model (min^{-1})
R^2	correlation coefficient
k_2	rate constant of pseudo-second order kinetic model (g mg^{-1} min^{-1})
α	rate constants
β	rate constants
nm	nanometer
μm	micrometer

respectively. Nitrate, EDTA and other chemicals of analytical grade were supplied by Sinopharm Chemical Reagent. Destilled-deionized water was used for all suspension or solution.

2.2. Preparation of nanofibrils

As described in our previous work (Liu, Wu, et al., 2011), raw chitosan powder (5 g) was poured into 1 L distilled deionized water to obtain a slurry. Stirred overnight, then the slurry was forced to pass through a wet-grinder (Labor-Pilot 2000/4, IKA Works, Inc.) equipped with a milling gap of about 0.1 mm at a flow speed of 10 L/h for 10 cycles. The thickened slurry was finally pumped through a high-pressure homogenizer (M-100P, Microfluidics Co., USA) for 10 cycles under a constant pressure of 250 MPa. The homogenized suspension composed of nanofibrils was freeze-dried for further characterizations and metal ion adsorption or desorption tests.

2.3. Adsorption

A batch equilibration method was used to determine sorption of metals. At room temperature, 100.0 mL metal ion solution with an initial concentration of 200 mg/L was buffered within the pH value of 5.0. Nanofibrillar chitosan (50.0 mg) was then poured into each metal ion solution and shaken in a thermostated shaker at 180 rpm. After a completely adsorption, the adsorbed metal ions/nanofibrils mixture was separated from suspensions by centrifugation (HC-2061, Anhui USTC Zonkia Scientific Instruments Co., China) at 12000 rpm. The concentrations of Cu(II), Pb(II) and Cd(II) ions in the supernatant were determined by flame atomic absorption spectroscopy (AAS) (3510G, Agilent Technologies Co., China) at wavelengths of 282.9, 324.4 and 228.4 nm, respectively.

Sorption capacity was tested by varying the sorption time (0–1500 min), initial concentration of metal ions (0–500 mg L^{-1}), and pH value of initial solution (2–5, adjusted by 0.1 M HNO_3 solution). Thermodynamic test was conducted at 20–70 °C under the sorption time of 4 h and pH at 5.0.

The competitive adsorption experiments of ternary metal ions were conducted by fixing the concentration of two ions at 50 mg/L, and then varied concentration of the 3rd ion from 25, 50, to 75 mg/L. The uptake amount of metal ions was calculated according to the following equation (Jeon & Ha Park, 2005):

$$q = \frac{(c_0 - c_e)V}{m} \quad (1)$$

2.4. Desorption and reuse

chitosan nanofibrils (50 mg) were poured into metal ion solutions (100 mL, 200 mg/L) and agitated for 24 h. Then the nanofibrils loaded with metal ions were collected, and gently washed with distilled-deionized water for 3 times to remove any unabsorbed ions. The sorption amount of ions was determined by AAS and calculated according to Eq. (1). For desorption studies, the adsorbents loaded with metal ions were poured into 100 mL EDTA solutions (0.01 M), thereby producing consecutive sorption and desorption for three cycles. The percentage of metal ions desorbed (D) was determined by AAS and calculated according to the following equation (Jeon & Ha Park, 2005):

$$D = \frac{q_d}{q} \times 100 \quad (2)$$

2.5. Characterization

Morphology of chitosan nanofibrils was carried out on a JEOL JEM 2010 FEF (UHR) Transmission Electron Microscope (TEM) with an accelerating voltage of 200 kV. Diluted suspensions of chitosan nanofibrils were spread out on the copper grids coated with carbon support film for observation. Surface morphology of nanofibrils and its complex chelated with metal ions was observed by a Scanning Electron Microscope (SEM) (SU1510, Hitachi Co.). The complex samples were subjected to calcination for 30 min at 350 or 500 °C, and then the resultant sinters were coated with gold for observation at 20 kV. The Brunauer–Emmett–Teller (BET) specific surface areas and total pore volume of nanofibrils were measured by nitrogen adsorption/desorption isotherm method using the Automated Gas Sorption (Autosorb-iQ-AG-MP, Quantachrome Co., USA). Fourier transform infrared spectroscopy (FTIR) (Nicolet Nexus 670, Thermo Electron Co., MA) of the samples was carried out in the range of 4000–750 cm^{-1} using the attenuated total reflection method at room temperature.

3. Results and discussion

3.1. Morphology and structure of nanofibrils and its chelation complex

TEM micrograph of chitosan nanofibrils as shown in Fig. 1a have diameter varied from 20 to 100 nm and exhibit a branch-shaped and cross-linked network. The BET surface area of chitosan nanofibrils was 20.503 m^2/g, three times higher than that of raw powder of chitosan (6.559 m^2/g), and the total pore volume was 0.011 cm^3/g for pore size smaller than 387.6 nm (diameter). Fig. 1b–e shows the micrographs of the sinter of metal ions loaded by nanofibrils calcinated at 300 and 500 °C. Pb(II) loaded chitosan nanofibrils calcinated at 300 °C shows a cross-linked and multi-porous network

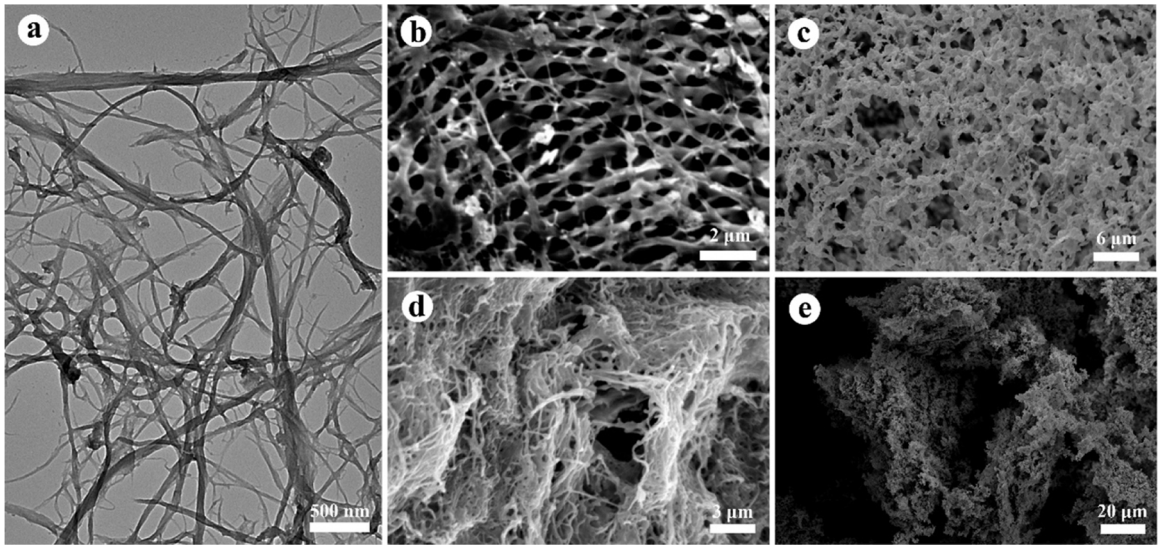

Fig. 1. TEM micrograph of chitosan nanofibrils (a), SEM micrographs of Pb(II) loaded nanofibrils sintered at 300 °C (b) and 500 °C (c), SEM micrographs of Cu(II) loaded nanofibrils sintered at 300 °C (d) and 500 °C (e).

with pore size varying from 0.35 to 2.5 μm, as well as the composite fibers with width ranged from 50 to 450 nm, larger than pure chitosan nanofibrils (Fig. 1b). It is also found that Cu(II) chelation complex sintered at 300 °C still present fibrillar network without any apparent particles on the fiber surface (Fig. 1d), indicating that the adsorption was not but a chemical one. The organic components were completely burned away at a sintering temperature of 500 °C (Fig. 1c and e). Grown inorganic compound of Pb still kept the fibrous morphology of fibrils but was enlarged diameter up to 0.12–1.2 μm. Copper compounds were grown into coralline granules and accumulated into fiber-like sinters. Above all, chemical chelation drove metal ions to deeply combine with nanofibrils, and the templet effects would be helpful for nucleation and growth of fine metal particles that could be retrieved by removing nanofibrillar chitosan.

The basic chemical structure of chitosan nanofibrils was characterized by FTIR spectra (not shown) which presented typical peaks of chitosan at 3434 cm^{-1} (–OH stretching vibrations), 3363 cm^{-1} (–NH stretching vibrations), 1654 cm^{-1} (the secondary amide C=O bond of the remaining acetamido groups), 1587 and 1421 cm^{-1} (–NH vibration and deformation in $–NH_2$), and 1087 and 1035 cm^{-1} (–CO stretching vibrations in –COH). While loading Cu(II), the peaks at 3434 and 1654 cm^{-1} strongly shifted to a lower wavenumber and –NH at 1421 cm^{-1} even disappeared, the fact revealed that the –OH may partly undergo adsorption and –NH may completely undergo adsorption with Cu(II). In the case of nanofibrils loaded with Cd(II) and Pb(II) ions, the relative intensity of –C=O at 1654 cm^{-1} compared to –NH vibration at 1587 cm^{-1} was elevated which may be due to the fact that –NH may undergo chelation of ions.

3.2. Effect of pH on adsorption capacity

Generally, as a polycationic carbohydrate, chelation of chitosan was greatly influenced by pH. Fig. 2a shows the effect of pH on the adsorption of Cu(II), Pb(II) and Cd(II) ions by nanofibrils. The adsorbed amount of metal ions increased with increasing pH, especially from 2.5 to 3.5, at pH 5.0, maximum uptakes were reached at the value of 164, 116, 61 mg/g, respectively, which were 8, 58, 3 times higher than that at pH 2.0. It was thought that in low acidic condition, the adsorbing sites of nanofibrils were mostly occupied by hydronium ions. With the rising of pH, the hydronium ions reduced and metal ions have competitive advantage to binding more metal ions (Wu, Tseng, & Juang, 1998).

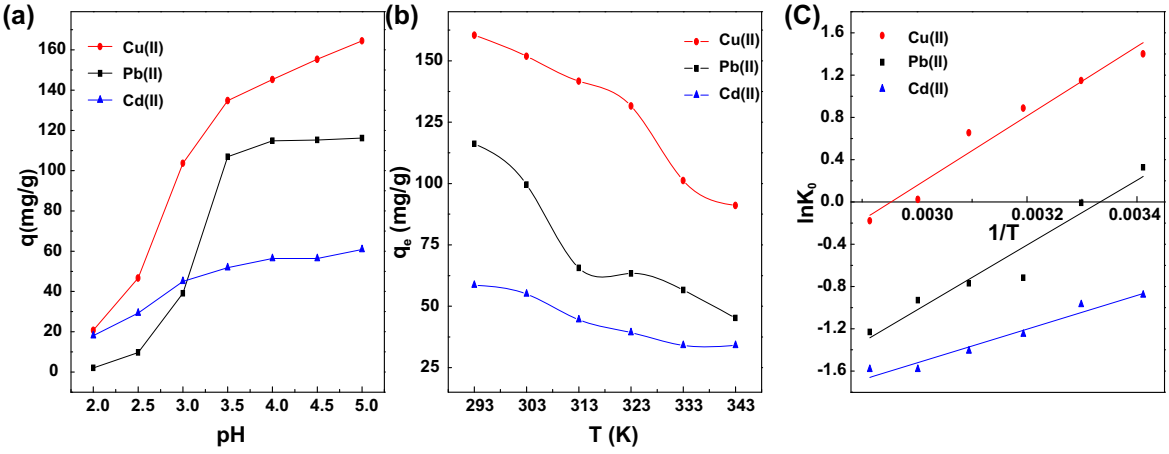

Fig. 2. Effects of pH and temperature on adsorption capacity of Cu(II), Pb(II) and Cd(II) ions chelated by chitosan nanofibrils (a and b); Plot of lnK_0 versus 1/T for estimation of thermodynamic parameters of adsorption (c).

Table 1
Thermodynamic parameters of Cu(II), Pb(II) and Cd(II) ions chelated by chitosan nanofibrils.

	Cu(II)	Pb(II)	Cd(II)
ΔG^0_{293} (kJ mol^{-1})	−0.71	0.49	2.61
ΔG^0_{303} (kJ mol^{-1})	−0.51	1.04	2.88
ΔG^0_{313} (kJ mol^{-1})	−0.24	2.44	3.61
ΔG^0_{323} (kJ mol^{-1})	0.05	2.63	4.10
ΔG^0_{333} (kJ mol^{-1})	1.08	3.08	4.66
ΔG^0_{343} (kJ mol^{-1})	1.51	3.90	4.80
ΔH^0 (kJ mol^{-1})	−14.16	−19.16	−11.57
ΔS^0 (J mol^{-1} K^{-1})	−45.13	−67.34	−48.25

(Experimental condition: volume = 100.0 mL; pH 5.0; [Cu(II), Pb(II) or Cd(II)] = 200 mg/L; adsorbent net mass = 50.0 mg; temperature = 20–70 °C; contact time = 4 h; Shaking rate = 180 rpm.)

3.3. Thermodynamic of adsorption

Fig. 2b shows the effect of temperature on uptake of Cu(II), Pb(II), and Cd(II) ions. A decreasing trend of ionic adsorption was displayed with increasing temperature from 20 to 70 °C. It was thought that the thermodynamic adsorption can be determined by the heat of adsorption at constant amount and the thermodynamic parameters of adsorption, i.e. ΔH^0, ΔG^0, and ΔS^0, were followed by the equations (Moradi, Aghaie, Zare, Monajjemi, & Aghaie, 2009):

$$\Delta G^0 = -RT \ln K_0 \quad (3)$$

$$K_0 = \frac{q_e}{c_e} \quad (4)$$

$$\ln K_0 = -\frac{\Delta H^0}{RT} + \frac{\Delta S^0}{R} \quad (5)$$

ΔG^0 was calculated by Eq. (3); the thermodynamic equilibrium constant K_0 was determined by Eq. (4) at different temperature; and values of ΔH^0 and ΔS^0 were obtained by fitting $\ln K_0 \sim T$ according to Eq. (5). The experimental or fitting results are indicated in Fig. 2c and summarized in Table 1. The ΔH^0 were determined as −14.16, −19.16, −11.57 kJ/mol, and the ΔS^0 were determined as −45.13, −67.34, −48.25 J mol^{-1} K^{-1} for chelation of Cu(II), Pb(II) and Cd(II) ions, respectively. The negative values of ΔH^0 indicates that the adsorption of all ions by nanofibrillar chitosan is exothermic, which is evidenced by increase in temperature. Wang et al. (2010) also reported that the formation of coordination complexes between metal cations and modified chitosan was exothermic in nature. Meanwhile, the negative values of ΔS^0 in this adsorption process identified the decreasing trend in the randomness at solid-solution interface during the ionic adsorption by chitosan nanofibrils. ΔG^0 indicates whether the adsorption process is spontaneous or not, e.g., a higher negative value reflects a more energetically favorable adsorption, therefore, negative ΔG^0 values at 293 K revealed that the adsorption process for Cu(II) ions was spontaneous. However, the value of ΔG^0 for all metal ions increased with the increment of temperature, indicating that the adsorption would be favorable at low temperatures because the nanofibrils were well dispersed at low temperature but aggregated at high temperature. Therefore, temperature is thought as one of the controllable factors in the exothermic adsorption process for nanofibrillar chitosan chelator (Foo & Hameed, 2010).

3.4. Adsorption equilibrium isotherm (single metal system)

Fig. 3a and b shows effects of the initial ionic concentration on uptake capacity and removal efficiency of metal ions. The adsorption capacity increased progressively to reach saturation with the increment of initial ionic concentration, whereas removal efficiency presented a converse trend. When the concentration of metal ion was lower than 20 mg/L, the removal efficiencies of Cu(II), Pb(II) and Cd(II) were about 90%, 60%, and 30%, respectively. The highest sorption efficiency of Cu(II) ion was ascribed to the excellent affinity of chitosan with Cu(II). The performance of adsorbate can be evaluated by maximum adsorption capacities q_m. The reported q_m of 5 different metal ions by several cross-linked or modified chitosan adsorbents are summarized and listed

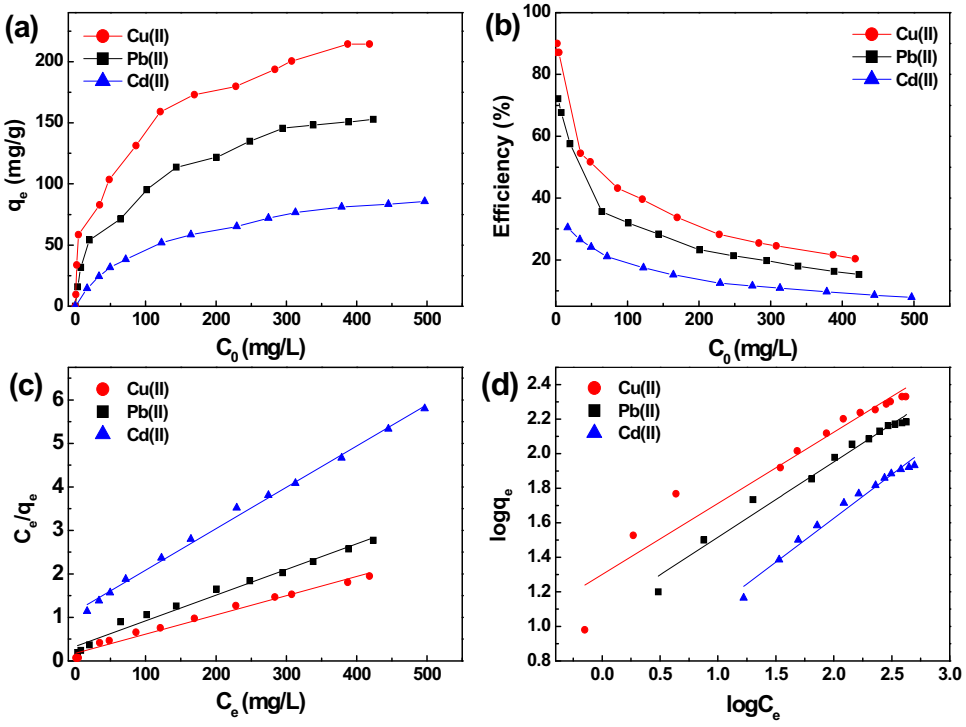

Fig. 3. Effects of initial ionic concentration on adsorption capacity (a) and efficiency (b) of chitosan nanofibrils; Langmuir (c) and Freundlich (d) models of Cu(II), Pb(II) and Cd(II) ions in single metal systems.

Table 2
Maximum adsorption capacity of various chitosan chelating agents for Cu(II), Pb(II), Cd(II), Zn(II), and Ni(II) ions.

Adsorbents	q_{max} (mg/g)				
	Cu(II)	Pb(II)	Cd(II)	Zn(II)	Ni(II)
Chitosan crosslinked with epichlorohydrin (Chen, Liu, Chen, & Chen, 2008)	35.5	34.1	–	10.2	–
Xanthate-modified magnetic chitosan (Zhu, Hu, & Wang, 2012)	34.5	76.9	–	20.8	–
Chitosan modified with complexation (Justi, Fávere, Laranjeira, Neves, & Peralta, 2005)	109	–	38.5	–	9.6
Modified magnetic chitosan chelating resin (Monier, Ayad, Wei, & Sarhan, 2010)	103.2	–	–	–	40.2
Chitosan/magnetite nanocomposite beads (Tran, Tran, & Nguyen, 2010)	–	63.3	–	–	52.6
Cross-linked magnetic chitosan-phenylthiourea (Monier & Abdel-Latif, 2012)	–	–	–	52.0	–
Chitin nanofibrils (Liu, Li, et al., 2013; Liu, Zhu, et al., 2013)	141.1	303.5	330.2	134.0	134.7
Chitosan nanofibrils (present work)	168.7	118.0	60.9	143.7	63.3

in Table 2 (Justi, Fávere, Laranjeira, Neves, & Peralta, 2005; Monier & Abdel-Latif, 2012; Monier, Ayad, Wei, & Sarhan, 2010; Tran, Tran, & Nguyen, 2010). In present work, the adsorption capacities of Cu(II), Pb(II), Cd(II), Zn(II), and Ni(II) on chitosan nanofibrils were 168.66, 118.00, 60.85, 143.67 and 63.32 mg/g, respectively, much higher than other reported chitosan adsorbents. It is thought that the excellent sorption performance was contributed to high specific area, widely distributed pores, and plenty of functional groups with good chelatability of nanofibril itself. It is interesting to make a comparison of sorption capacity between nanofibrillar chitosan and nanofibrillar chitin (Liu, Li, et al., 2013). It is true that the former has a favorable Cu(II) and Zn(II) uptake perhaps because of the difference of chelation between $-NH_2$ and $-NHCOCH_3$.

Langmuir or Freundlich models are normally used adsorption isotherms. The former one assume that the adsorbent surface has sites of identical energy and each adsorbate molecule located at a single site; hence, it predicts the formation of adsorbate monolayer on the adsorption surface (Liu, Li, et al., 2013; Vijayaraghavan, Padmesh, Palanivelu, & Velan, 2006). This model preferentially used in studies on adsorption in solution and the linear form is represented by Eq. (6).

$$\frac{c_e}{q_e} = \frac{1}{K_L q_m} + \frac{c_e}{q_m} \tag{6}$$

K_L was employed to determine the q_m and K_L values from the angular and linear coefficients obtained by plotting. R_L calculated by K_L, is a dimensionless separation factor defined by Webi and Chakravort (1974), and is expressed as follows:

$$R_L = \frac{1}{1 + K_L c_0} \tag{7}$$

The values R_L indicate whether the adsorption is irreversible ($R_L = 0$), favorable ($0 < R_L < 1$), linear ($R_L = 1$) or unfavorable ($R_L > 1$) (Laus & de Fávere, 2011).

The Freundlich isotherm is the earliest equation describing the non-ideal and reversible adsorption, and one of the most widely used isotherms for the description of multi-site adsorption (Adamson & Gast, 1997). Mathematically, it can be expressed in the linearized logarithmic form as:

$$\log q_e = \log K_F + \frac{1}{n} \log c_e \tag{8}$$

Fig. 3c and d shows the fitting plots based on Langmuir and Freundlich models for sorption of Cu(II), Pb(II), and Cd(II). The calculated Langmuir and Freundlich parameters are presented in Table 3. In Langmuir isotherm, K_L of Cu(II), related to the affinity of binding sites (Ngah & Fatinathan, 2010), showed the highest value among three ions. The R_L values lies in the range of $0 < R_L < 1$, indicating that the adsorption of Cu(II), Pb(II) and Cd(II) ions by nanofibrils is favorable in single metal system. However, the value of calculated q_m of metal ions at monolayer was much higher than measured q_m. Based on Freundlich model, K_F obtained for Cu(II) ions was higher than the others. The parameter n or $1/n$ value is related to the degree of surface heterogeneity. If $1/n$ value is close to 1 or even 1, the adsorbent is indicated to have relatively more homogeneous binding sites (Deng, Liu, Zeng, Qiu, & Li, 2013). The $1/n$ values obtained for Cu(II), Pb(II) and Cd(II) ions were 0.4121, 0.4361, and 0.5071, respectively, indicating that for the adsorption of Cu(II), Pb(II) and Cd(II) ions on the solid–liquid interface, the binding sites involved were more of heterogeneous nature. Based on the correlation coefficients-R^2 of these two models, the adsorption correlated better with Langmuir than Freundlich isotherm model.

3.5. Adsorption kinetics

The profiles of metal ion uptake versus time always begin with a rapid phase followed by a relatively slow phase (Liu & Cheng, 2012). In this work, the sorption curve in Fig. 4a displays a similar trend, that is, the q_t increased very fast in 60 min, and then slowly arrived to equilibrium, and lastly remained constant after 120 min.

Several models such as pseudo-first order kinetic, pseudo-second order kinetic, intraparticular models have been used to describe the adsorption kinetics and the rate limited step during adsorption process, which include diffusion control, chemical reaction and particle diffusion, etc. The pseudo-first order kinetic model is given as (Wu, Tseng, & Juang, 2001).

$$\log(q_e - q_t) = \log q_e - \frac{k_1}{2.303} t \tag{9}$$

While the pseudo-second order kinetic model was expressed as follow (Ho, 2006):

$$\frac{t}{q_t} = \frac{1}{k_2 q_e^2} + \frac{t}{q_e} \tag{10}$$

The straight-line plots of $\log(q_e - q_t)$ against t were used to determine the k_1 and correlation coefficient R^2, and the straight-line plots of t/q_t against t were used to determine the k_2 and correlation coefficient R^2.

Table 3
Langmuir and Freundlich isotherm parameters for metal ions chelated by chitosan nanofibrils.

		Cu(II)	Pb(II)	Cd(II)
Measured q_m (mg/g)		168.66	118.00	60.85
Langmuir	q_m (mg/g)	227.27	169.49	105.26
	K_L (L/mg)	0.0253	0.0176	0.0083
	R_L	0.88–0.07	0.84–0.10	0.83–0.18
	R^2	0.9829	0.9842	0.9964
Freundlich	$1/n$	0.4121	0.4361	0.5071
	K_F (mg/g)	19.9664	12.0337	4.0917
	R^2	0.9310	0.9794	0.9807

(Experimental condition: volume = 100.0 mL; pH 5.0; [Cu(II), Pb(II) or Cd(II)] = 10–500 mg/L; adsorbent net mass = 50.0 mg; temperature = 20 °C; contact time = 4 h; shaking rate = 180 rpm.)

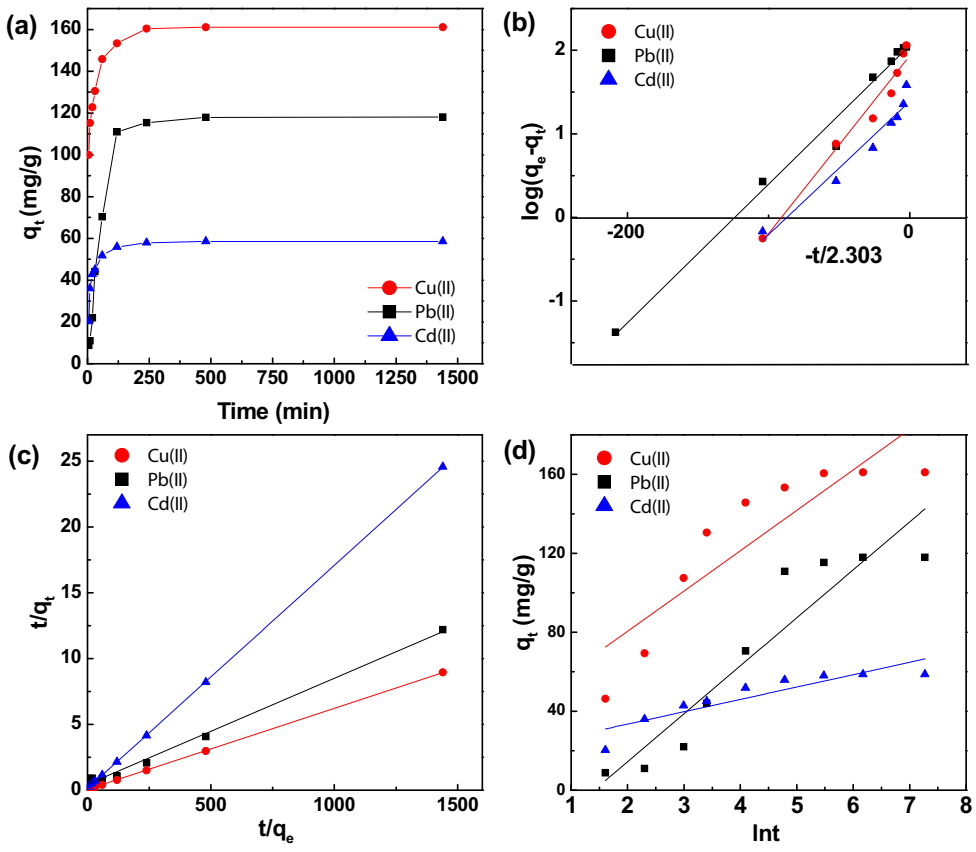

Fig. 4. Profiles of adsorption kinetic of Pb(II), Cu(II) and Cd(II) ions chelated by chitosan nanofibrils in single metal ion system. Adsorption capacity versus contact time (a), pseudo-first order plot (b), pseudo-second order plot (c), and Elovich plot (d).

If the process is a chemical sorption, the sorption kinetics could be modeled by Elovich equation (Chien & Clayton, 1980):

$$q_t = \frac{1}{\beta}\ln(\alpha+\beta) + \frac{1}{\beta}\ln t \quad (11)$$

The Elovich equation allows establishing if the process is based on diffusion or chemical reaction control.

Three possible kinetic models were shown in Fig. 4c–e and the parameters calculated were listed in Table 4. Although the results of the plot of the pseudo-first order kinetic model was linear, the $q_{e\,(theor.)}$ value of Cu(II) and Cd(II) was not in agreement with $q_{e\,(exp.)}$, indicating a poor fit for pseudo-first order kinetic model (Ma, Wu, Guo, Zhang, & Ma, 2013). Moreover, this model could not be perfectly applicable over the initial stage of the adsorption process, but the pseudo-second order kinetic model could predict the behavior over the whole range of contact time. Correlation coefficient R^2 from pseudo-second order model is higher than 0.99, and more closer to 1 than pseudo-first order model and Elovich model. Therefore, the ion sorption kinetic for nanofibrils was preferable to fitting pseudo-second order model which always described the chemisorptions involved valence forces through sharing or exchange of electrons between metal ions and the adsorbent (Hasan, Ahmad, & Hameed, 2008).

Table 4
Kinetic parameters of three sorption models.

		Cu(III)	Pb(II)	Cd(II)
$q_{e(exp)}$ (mg/g)	168.66	118.00	60.85	
Pseudo-first order model	R^2	0.9695	0.9862	0.9515
	k_1 (min^{-1})	0.0213	0.0166	0.0159
	$q_{e\,(theor)}$ (mg/g)	85.74	113.55	24.40
Pseudo-second order model	R^2	0.9999	0.9953	1.0000
	k_2 (g mg^{-1} min^{-1})	0.0008	0.0001	0.0024
	$q_{e\,(theor)}$ (mg/g)	161.29	123.46	58.82
Elovich model	R^2	0.7902	0.8838	0.8094
	α (mg g^{-1} min^{-1})	66.2976	5.9476	177.0021
	β (g/mg)	0.0253	0.0412	0.1597

(Experimental condition: volume = 100.0 mL; pH 5.0; [Cu(II), Pb(II) or Cd(II)] = 200 mg/L; adsorbent net mass = 50.0 mg; temperature = 20 °C; contact time = 5 min – 24 h; shaking rate = 180 rpm.)

3.6. Competitive adsorption

In nature systems, numerous metal ions are often present together to form multi-component solutions (Chen, 2008; Laus, 2011). As discussed above, Cu(II) showed a higher affinity to nanofibrils than the others in a single metal system. In a ternary metal ion system, the results from competitive adsorption are shown in Fig. 5. The uptake capacity of Cu(II), Pb(II) and Cd(II) increased with the increment of each concentration because of the increasing chances of competition. Interestingly, to increase the concentration of Pb(II) ion would synergetically enhanced the chelation of Cu(II) and Cd(II) ions. Fig. 5b, d and f shows the effect of ionic concentration on removal efficiency in ternary metal ion system. Cu(II) was the most competitive ion and restrained the removal of the other ions, whose removal is over 60%. On the other hand, removal efficiency of Cd(II) ion was lowest among three metal ions.

3.7. Desorption

Normally, desorption experiments have been conducted by using HNO_3, H_2SO_4, EDTA and HCl solutions as desorbents (Ngah & Fatinathan, 2010). In this work, nanofibrils could not be dissolved

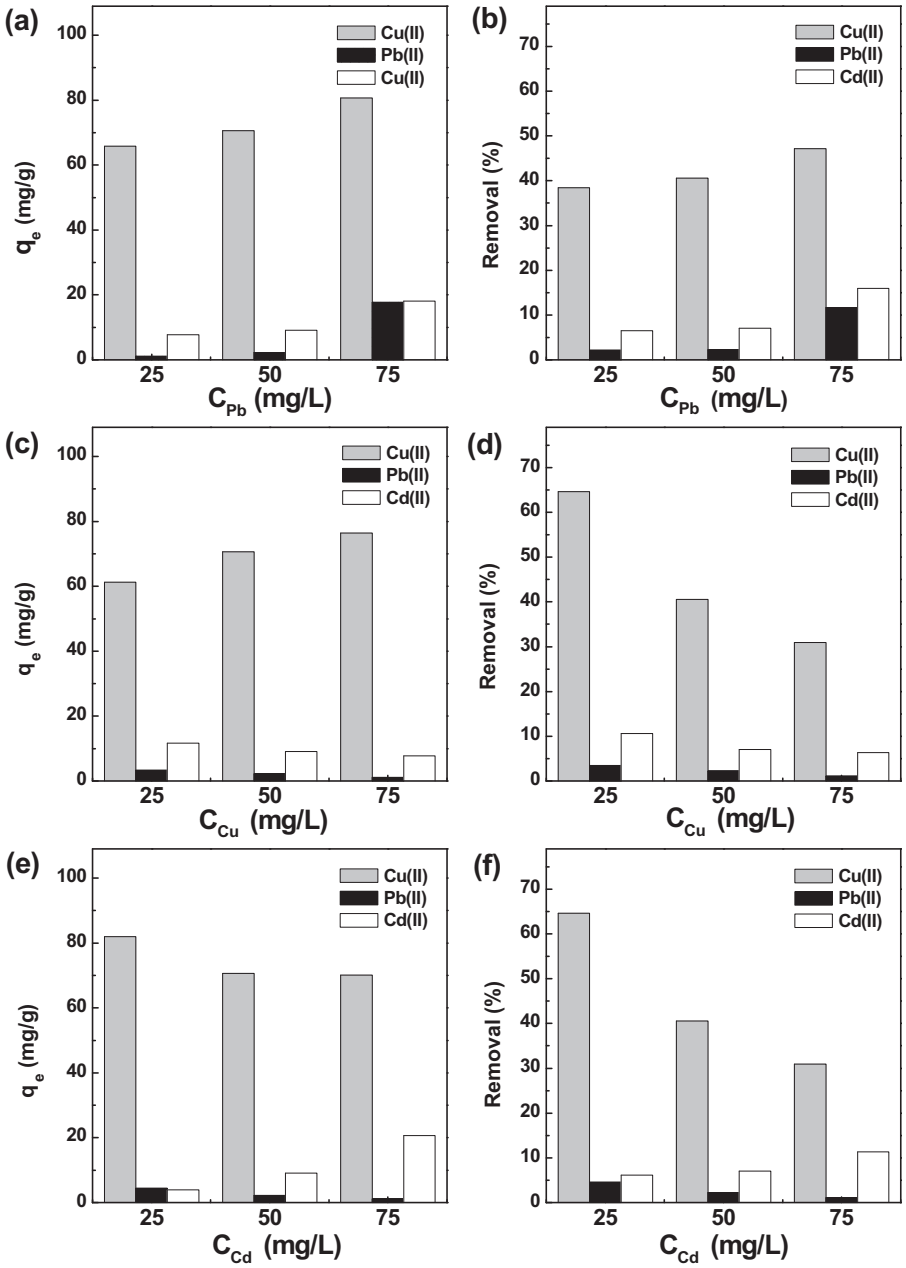

Fig. 5. Competitive adsorption capacity and removal of Cu(II), Pb(II) and Cd(II) ions chelated by chitosan nanofibrils in ternary metal ions system. (Experimental condition: Cu(II), Pb(II) or Cd(II) = 25.0–75.0 mg/L, other two metal ions = 50.0 mg/L; adsorbent net mass = 50.0 mg.).

in EDTA but in acid media, therefore EDTA was preferably used as a desorbent. The desorption and recovery percentage of Cu(II), Pb(II) and Cd(II) ions desorbed from the eluent in three consecutive cycles are shown in Table 5. There was a reduction (about 2%) of q_e of Cu(II), Pb(II) and Cd(II) ions desorbed from the first to second cycle, but the amount of desorption have little change after three cycles. The desorption percentage for Pb(II), Cu(II) and Cd(II) ions could be improved by increasing the concentration of EDTA, e.g., the desorption values of Cu(II), Pb(II) and Cd(II) complex in 0.01 M EDTA were 72.6%, 81.2% and 84.4%, respectively, whereas the maximum desorption capacities of Cu(II), Pb(II), Cd(II) ions in 0.1 M EDTA solution were increased up to 77.9, 87.1, and 89.9 mg/g,

Table 5
Desorption percentage and recovery of Cu(II), Pb(II) and Cd(II) ions desorbed for three cycles in 0.01 M EDTA solution.

Metal ions	Desorption (%)						Medium (EDTA)	Recovery (%)		
	0.005	0.01	0.02	0.03	0.05	0.10		Cycle 1	Cycle 2	Cycle 3
Cu(II)	70.4	81.2	83.5	85.1	86.2	87.1	0.01 M	72.6	71.4	73.3
Pb(II)	55.7	72.6	74.5	76.2	77.1	77.9		81.2	80.3	80.2
Cd(II)	79.1	84.4	86.2	88.1	89.0	89.9		84.4	81.7	82.7

respectively. It is meaningful that the desorption capacity of ions are opposite to their sorption capacity (Gu, Schmitt, Chen, Liang, & McCarthy, 1994; Laus & de Fávere, 2011). For instance, among three ions, Cu(II) ion had the highest sorption capacity but the lowest desorption percentage because of its strong selectivity of sorption by chitosan nanofibrils. On the contrary, Cd(II) ion presented lowest adsorption capacity but the highest desorption.

4. Conclusions

In this work, nanofibrillar chitosan as a highly efficient metal ion chelator, was beneficial from its cross-linked, porous morphology and plenty of chelating groups. Its q_{max} was much higher than reported chitosan chelating agents. Meanwhile, q_e was highly dependent on pH value, temperature, initial ionic concentration, and time because the adsorption was exothermic and correlated to Langmuir isotherm and the pseudo-second order thermodynamic model. The recycled nanofibrils could be obtained at about 80% recovery level on desorbing metal ions after 3 cycles. Cu(II) presented the highest q_e but lowest desorption amount among three metal ions, indicating a high sorption selectivity by chitosan nanofibrils.

Acknowledgements

The authors are grateful to National Natural Science Foundation of China (Nos. 21277073 and 51103073), Natural Science Foundation of Jiangsu Province (No. BK2011828), Scientific Research Foundation for the Returned Overseas Chinese Scholars, and Qing Lan Project and Six Talented Peak Program of Jiangsu Province and the Priority Academic Program Development of Jiangsu Higher Education Institutions for financial support. Support Program of key project of outstanding undergraduate thesis (design) from Nanjing University of Information Science & Technology are also acknowledged.

References

Adamson, A. W., & Gast, A. P. (1997). *Physical chemistry of surfaces* (6th ed.). New York: Wiley Interscience.
Chen, A.-H., Liu, S.-C., Chen, C.-Y., & Chen, C.-Y. (2008). Comparative adsorption of Cu(II), Zn(II), and Pb(II) ions in aqueous solution on the crosslinked chitosan with epichlorohydrin. *Journal of Hazardous Materials*, *154*, 184–191.
Chien, S. H., & Clayton, W. R. (1980). Application of Elovich equation to the kinetics of phosphate release and sorption in soils. *Soil Science Society of America Journal*, *44*, 265–268.
Deng, P., Liu, W., Zeng, B., Qiu, Y., & Li, L. (2013). Sorption of heavy metals from aqueous solution by dehydrated powders of aquatic plants. *International Journal of Environmental Science and Technology*, *10*, 559–566.
Foo, K. Y., & Hameed, B. H. (2010). Insights into the modeling of adsorption isotherm systems. *Chemical Engineering Journal*, *156*, 2–10.
Gamage, A., & Shahidi, F. (2007). Use of chitosan for the removal of metal ion contaminants and proteins from water. *Food Chemistry*, *104*, 989–996.
Gu, B., Schmitt, J., Chen, Z., Liang, L., & McCarthy, J. F. (1994). Adsorption and desorption of natural organic matter on iron oxide: Mechanisms and models. *Environmental Science & Technology*, *28*, 38–46.
Haider, S., & Park, S.-Y. (2009). Preparation of the electrospun chitosan nanofibers and their applications to the adsorption of Cu(II) and Pb(II) ions from an aqueous solution. *Journal of Membrane Science*, *328*, 90–96.
Hasan, M., Ahmad, A. L., & Hameed, B. H. (2008). Adsorption of reactive dye onto cross-linked chitosan/oil palm ash composite beads. *Chemical Engineering Journal*, *136*, 164–172.
Ho, Y.-S. (2006). Review of second-order models for adsorption systems. *Journal of Hazardous Materials*, *136*, 681–689.
Jeon, C., & Ha Park, K. (2005). Adsorption and desorption characteristics of mercury(II) ions using aminated chitosan bead. *Water Research*, *39*, 3938–3944.
Justi, K. C., Fávere, V. T., Laranjeira, M. C. M., Neves, A., & Peralta, R. A. (2005). Kinetics and equilibrium adsorption of Cu(II), Cd(II), and Ni(II) ions by chitosan functionalized with 2[-bis-(pyridylmethyl)aminomethyl]-4-methyl-6-formylphenol. *Journal of Colloid and Interface Science*, *291*, 369–374.
Laus, R., & de Fávere, V. T. (2011). Competitive adsorption of Cu(II) and Cd(II) ions by chitosan crosslinked with epichlorohydrin–triphosphate. *Bioresource Technology*, *102*, 8769–8776.
Liu, D., Chang, P. R., Chen, M., & Wu, Q. (2011). Chitosan colloidal suspension composed of mechanically disassembled nanofibers. *Journal of Colloid and Interface Science*, *354*, 637–643.
Liu, Y. Z., & Cheng, J. M. (2012). Adsorption kinetics and isotherms of Cu (II) and Cd (II) onto oxidized nano carbon black. *Advanced Materials Research*, *529*, 579–584.
Liu, D., Li, Z., Li, W., Zhong, Z., Xu, J., Ren, J., et al. (2013). Adsorption behavior of heavy metal ions from aqueous solution by soy protein hollow microspheres. *Industrial & Engineering Chemistry Research*, *52*, 11036–11044.
Liu, D., Wu, Q., Chang, P. R., & Gao, G. (2011). Self-assembled liquid crystal film from mechanically defibrillated chitosan nanofibers. *Carbohydrate Polymers*, *84*, 686–689.
Liu, D., Zhu, Y., Li, Z., Tian, D., Chen, L., & Chen, P. (2013). Chitin nanofibrils for rapid and efficient removal of metal ions from water system. *Carbohydrate Polymers*, *98*, 483–489.
Ma, X. H., Wu, L. M., Guo, X. Y., Zhang, M. H., & Ma, A. L. (2013). Methylene blue adsorption by synthetic nano-carbon-hydroxylapatite. *Advanced Materials Research*, *664*, 326–330.
Monier, M., & Abdel-Latif, D. A. (2012). Preparation of cross-linked magnetic chitosan-phenylthiourea resin for adsorption of Hg(II), Cd(II) and Zn(II) ions from aqueous solutions. *Journal of Hazardous Materials*, *209–210*, 240–249.
Monier, M., Ayad, D. M., Wei, Y., & Sarhan, A. A. (2010). Adsorption of Cu(II), Co(II), and Ni(II) ions by modified magnetic chitosan chelating resin. *Journal of Hazardous Materials*, *177*, 962–970.
Moradi, O., Aghaie, M., Zare, K., Monajjemi, M., & Aghaie, H. (2009). The study of adsorption characteristics Cu^{2+} and Pb^{2+} ions onto PHEMA and P(MMA-HEMA) surfaces from aqueous single solution. *Journal of Hazardous Materials*, *170*, 673–679.
Muzzarelli, R. A. A. (1973). *Natural chelating polymers*. Oxford: Pergamon Press.
Muzzarelli, R. A. A. (2011). Potential of chitin/chitosan-bearing materials for uranium recovery: An interdisciplinary review. *Carbohydrate Polymers*, *84*, 54–63.
Muzzarelli, R. A. A. (2012). Nanochitins and nanochitosans, paving the way to eco-friendly and energy-saving exploitation of marine resources. *Polymer Science: A Comprehensive Reference*, *10*, 153–164.
Muzzarelli, R. A. A., Ferrero, A., & Pizzoli, M. (1972). Light-scattering, x-ray diffraction, elemental analysis and infrared spectrometry characterization of chitosan a chelating polymer. *Talanta*, *19*, 1222–1226.
Muzzarelli, R. A. A., & Sipos, L. (1971). Chitosan for the collection from seawater of naturally occurring zinc, cadmium, lead and copper. *Talanta*, *28*, 838–853.
Ngah, W., & Fatinathan, S. (2010). Adsorption characterization of Pb (II) and Cu (II) ions onto chitosan-tripolyphosphate beads: Kinetic, equilibrium and thermodynamic studies. *Journal of Environmental Management*, *91*, 958.
Popuri, S. R., Vijaya, Y., Boddu, V. M., & Abburi, K. (2009). Adsorptive removal of copper and nickel ions from water using chitosan coated PVC beads. *Bioresource Technology*, *100*, 194–199.
Tran, H. V., Tran, L. D., & Nguyen, T. N. (2010). Preparation of chitosan/magnetite composite beads and their application for removal of Pb(II) and Ni(II) from aqueous solution. *Materials Science and Engineering C*, *30*, 304–310.
Vijayaraghavan, K., Padmesh, T. V. N., Palanivelu, K., & Velan, M. (2006). Biosorption of nickel (II) ions onto *Sargassum wightii*: Application of two-parameter and three-parameter isotherm models. *Journal of Hazardous Materials*, *133*, 304–308.
Wang, L., Xing, R., Liu, S., Qin, Y., Li, K., Yu, H., et al. (2010). Studies on adsorption behavior of Pb(II) onto a thiourea-modified chitosan resin with Pb(II) as template. *Carbohydrate Polymers*, *81*, 305–310.
Wan Ngah, W. S., Teong, L. C., & Hanafiah, M. A. K. M. (2011). Adsorption of dyes and heavy metal ions by chitosan composites: A review. *Carbohydrate Polymers*, *83*, 1446–1456.
Webi, T. W., & Chakravort, R. K. (1974). Pore and solid diffusion models for fixed-bed adsorbers. *AIChE Journal*, *20*, 228–238.
Wu, F.-C., Tseng, R.-L., & Juang, R.-S. (1998). Role of pH in metal adsorption from aqueous solutions containing chelating agents on chitosan. *Industrial & Engineering Chemistry Research*, *38*, 270–275.
Wu, F.-C., Tseng, R.-L., & Juang, R.-S. (2001). Kinetic modeling of liquid-phase adsorption of reactive dyes and metal ions on chitosan. *Water Research*, *35*, 613–618.
Zhu, Y., Hu, J., & Wang, J. (2012). Competitive adsorption of Pb(II), Cu(II) and Zn(II) onto xanthate-modified magnetic chitosan. *Journal of Hazardous Materials*, *221-222*, 155–161.